

Contribution from the Departments of Chemistry, University of Notre Dame, Notre Dame, Indiana 46556, and University of Southern California, Los Angeles, California 90089-1062, and Department of Physics, Pennsylvania State University, University Park, Pennsylvania 16802

## On the Preparation of Five-Coordinate (3-Chloropyridine)(porphinato)iron(III) Complexes

W. Robert Scheidt,\*<sup>1</sup> David K. Geiger,<sup>1</sup> Young Ja Lee,<sup>1</sup> Christopher A. Reed,\*<sup>2</sup> and G. Lang\*<sup>3</sup>

Received October 2, 1986

The preparation of two crystalline species,  $[\text{Fe}(\text{OEP})(3\text{-Cl-py})]\text{ClO}_4$  and  $[\text{Fe}(\text{OEP})(3\text{-Cl-py})_2]\text{ClO}_4$ , in the reaction of equimolar quantities of  $[\text{Fe}(\text{OEP})(\text{OCIO}_3)]$  and 3-chloropyridine is reported. The six-coordinate byproduct occurs even when the starting iron(III) porphyrinate is in excess. Both species have been characterized by X-ray structure determinations. The crystalline five-coordinate complex can be separated from the six-coordinate species by differential flotation; the resulting pure complex has also been characterized by temperature-dependent magnetic susceptibilities and Mössbauer spectroscopy. Both isolated species are best described as admixed intermediate-spin compounds.  $[\text{Fe}(\text{OEP})(3\text{-Cl-py})]\text{ClO}_4$  has an average Fe-N<sub>p</sub> distance of 1.979 (6) Å and an axial Fe-N<sub>py</sub> distance of 2.126 (5) Å. The iron(III) atom is displaced by 0.22 Å from the mean plane of the core. The  $[\text{Fe}(\text{OEP})(3\text{-Cl-py})]^{+}$  ions interact in pairs via a  $\pi$ - $\pi$  interaction.  $[\text{Fe}(\text{OEP})(3\text{-Cl-py})_2]\text{ClO}_4$  has an average Fe-N<sub>p</sub> distance of 2.006 (8) Å and an average axial Fe-N<sub>py</sub> bond distance of 2.304 Å. Crystal data for  $[\text{Fe}(\text{OEP})(3\text{-Cl-py})]\text{ClO}_4$ :  $\text{FeCl}_2\text{O}_4 \cdot \text{N}_5\text{C}_4\text{H}_4$ , monoclinic, space group  $C2/c$ ,  $a = 18.754$  (12) Å,  $b = 16.160$  (9) Å,  $c = 27.350$  (15) Å,  $\beta = 103.97$  (4)°,  $Z = 8$ , 4800 unique observed data. Crystal data for  $[\text{Fe}(\text{OEP})(3\text{-Cl-py})_2]\text{ClO}_4$ :  $\text{FeCl}_2\text{O}_4 \cdot \text{N}_6\text{C}_8\text{H}_8$ , orthorhombic, space group  $Pbca$ ,  $a = 26.171$  (6) Å,  $b = 38.014$  (8) Å,  $c = 10.020$  (2) Å,  $Z = 8$ , 4593 unique observed data. All data were collected at 292 K with use of Mo  $K\alpha$  radiation.

We have recently<sup>4</sup> reported the preparation and characterization of  $[\text{Fe}(\text{OEP})(2\text{-MeHIm})]\text{ClO}_4$ .<sup>5</sup> This five-coordinate high-spin ferric porphyrinate has the neutral nitrogen donor 2-methylimidazole as the axial ligand rather than the usual anion typical<sup>6</sup> of five-coordinate ferric species. This complex was prepared by the addition of an equimolar quantity of the imidazole to  $[\text{Fe}(\text{OEP})(\text{OCIO}_3)]$ . This synthetic method, i.e., reaction of equimolar quantities of a neutral ligand and a ferric porphyrinate, yields species with mono(neutral ligand) stoichiometry in some instances<sup>7</sup> but bis(ligand) complexes in other cases.<sup>8</sup> Our crystal structure analysis of  $[\text{Fe}(\text{OEP})(2\text{-MeHIm})]\text{ClO}_4$ <sup>4</sup> suggested a rational explanation for the dichotomy of products obtained by using this approach. Two different crystalline modifications of  $[\text{Fe}(\text{OEP})(2\text{-MeHIm})]\text{ClO}_4$  were both found to display a  $\pi$ - $\pi$  interaction between pairs of  $[\text{Fe}(\text{OEP})(2\text{-MeHIm})]^{+}$  ions that effectively blocks the sixth coordination site. Thus this formation of  $\pi$ - $\pi$  dimers was suggested<sup>4</sup> as the most important factor that allowed the isolation of five-coordinate rather than six-coordinate species.<sup>9</sup> Such  $\pi$ - $\pi$  dimers are readily possible with some porphyrin ligands, i.e.,  $\text{H}_2\text{OEP}$  and other porphyrins with alkyl peripheral substituents, but much less with porphyrins having bulkier peripheral groups, i.e.,  $\text{H}_2\text{TPP}$ .

We have been exploring the generality of this synthetic approach to prepare five-coordinate ferric porphyrinates with neutral axial ligands. In particular, we wished to compare a less sterically hindered pyridine derivative with the 2-methylimidazole derivative to explore the effects of the sterically important 2-methyl substituent on the formation of the five-coordinate complex. We

report herein the products of the reaction of equimolar quantities of 3-chloropyridine and  $[\text{Fe}(\text{OEP})(\text{OCIO}_3)]$ . In our hands, two crystalline products are always obtained: a five-coordinate and a six-coordinate complex. The presence of both  $[\text{Fe}(\text{OEP})(3\text{-Cl-py})]\text{ClO}_4$  and  $[\text{Fe}(\text{OEP})(3\text{-Cl-py})_2]\text{ClO}_4$  in all preparations has been established by X-ray structure determinations. The structure determinations show that both species have stereochemistries consistent<sup>6</sup> with admixed intermediate-spin states. The current crystals of  $[\text{Fe}(\text{OEP})(3\text{-Cl-py})_2]\text{ClO}_4$  are the third crystalline modification of this six-coordinate complex to be isolated and characterized. The first<sup>10</sup> was found to be a thermal spin equilibrium ( $S = 5/2$ ,  $S = 1/2$ ), while the second modification,<sup>11</sup> an apparently metastable phase, was found to have an admixed intermediate-spin state. The isolation of this third crystalline phase confirms the suggestion<sup>11,12</sup> that the three possible spin states of six-coordinate ferric porphyrinates have relatively similar energies under some conditions. This similarity in spin-state energy can now also be applied to neutral-axial-ligand five-coordinate compounds.  $[\text{Fe}(\text{OEP})(3\text{-Cl-py})]\text{ClO}_4$  is an intermediate-spin-state complex, while  $[\text{Fe}(\text{OEP})(2\text{-MeHIm})]\text{ClO}_4$ <sup>4</sup> is a high-spin complex. In addition, a number of intermediate-spin species carrying an anionic axial ligand have been reported.<sup>8,13,14</sup>

$[\text{Fe}(\text{OEP})(3\text{-Cl-py})]^{+}$  ions are found to form  $\pi$ - $\pi$  dimers in the solid state; however, the tightness of the interaction is less than that found in crystalline  $[\text{Fe}(\text{OEP})(2\text{-MeHIm})]\text{ClO}_4$ . Nonetheless, the formation of  $\pi$ - $\pi$  dimers affects the detailed magnetic susceptibility in the solid state.

### Experimental Section

**Synthesis and Physical Characterization.** Single crystals of the complexes were grown by slow vapor diffusion of hexane into a chloroform solution containing equimolar amounts of 3-chloropyridine and  $[\text{Fe}(\text{OEP})(\text{OCIO}_3)]$ .<sup>15</sup> A typical preparation is as follows: 73 mg of  $[\text{Fe}(\text{OEP})(\text{OCIO}_3)]$  (0.102 mmol) was put into 5.0 mL of 0.021 M 3-chloropyridine (0.105 mmol) in  $\text{CHCl}_3$ . This solution was divided into four parts, and each portion (in 5-mL beakers) was set over a 2/1 hexane/chloroform mixture. After 3 or 4 days, black single crystals of both complexes as well as a smaller amount of amorphous or microcrystalline

- (1) University of Notre Dame.
- (2) University of Southern California.
- (3) Pennsylvania State University.
- (4) Scheidt, W. R.; Geiger, D. K.; Lee, Y. J.; Reed, C. A.; Lang, G. *J. Am. Chem. Soc.* **1985**, *107*, 5693-5699.
- (5) Abbreviations used in this paper: OEP and TPP, the dianions of octaethylporphyrin and meso-tetraphenylporphyrin, respectively; 2-MeHIm, 2-methylimidazole; 3-Cl-py, 3-chloropyridine; N<sub>p</sub>, porphinato nitrogen atom; N<sub>py</sub>, 3-chloropyridine nitrogen atom; Ct, center of the porphyrin ring.
- (6) Scheidt, W. R.; Reed, C. A. *Chem. Rev.* **1981**, *81*, 543-555.
- (7) (a) Ogoshi, H.; Watanabe, E.; Yoshida, Z. *Chem. Lett.* **1973**, 989-992. (b) Ogoshi, H.; Sugimoto, H.; Watanabe, E.; Yoshida, Z.; Maeda, Y.; Sakai, H. *Bull. Chem. Soc. Jpn.* **1981**, *54*, 3414-3419. (c) Yoshimura, T.; Ozaki, T.; Shintani, Y.; Watanabe, H. *J. Inorg. Nucl. Chem.* **1976**, *38*, 1879-1883. (d) Yoshimura, T.; Ozaki, T.; Shintani, Y. *J. Inorg. Nucl. Chem.* **1977**, *39*, 185-190.
- (8) Reed, C. A.; Mashiko, T.; Bentley, S. P.; Kastner, M. E.; Scheidt, W. R.; Spartalian, K.; Lang, G. *J. Am. Chem. Soc.* **1979**, *101*, 2948-2958.
- (9) In principle, a six-coordinate species could be formed by coordination of two neutral ligands or by the retention of the coordinated anion after addition of the neutral axial ligand. This latter possibility was not eliminated in any of the earlier work.<sup>7</sup>

- (10) Scheidt, W. R.; Geiger, D. K.; Haller, K. *J. Am. Chem. Soc.* **1982**, *104*, 495-499.
- (11) Scheidt, W. R.; Geiger, D. K.; Hayes, R. G.; Lang, G. *J. Am. Chem. Soc.* **1983**, *105*, 2625-2632.
- (12) Scheidt, W. R.; Gouterman, M. In *Physical Bioinorganic Chemistry: Iron Porphyrins*; Lever, A. B. P., Gray, H. B., Eds.; Addison-Wesley: Reading, MA, 1983; Part I, pp 89-139.
- (13) Masuda, H.; Taga, T.; Osaki, K.; Sugimoto, H.; Yoshida, S.-I.; Ogoshi, H. *Inorg. Chem.* **1980**, *19*, 950-955.
- (14) Shelly, K.; Bartczak, T.; Scheidt, W. R.; Reed, C. A. *Inorg. Chem.* **1985**, *24*, 4325-4330.
- (15) Dolphin, D. H.; Sams, J. R.; Tsin, T. B. *Inorg. Chem.* **1977**, *16*, 711-713.

**Table I.** Summary of Crystal Data and Intensity Collection Parameters

	[Fe(OEP)(3-Cl-py) <sub>2</sub> ]ClO <sub>4</sub> ·CHCl <sub>3</sub>	[Fe(OEP)(3-Cl-py)]ClO <sub>4</sub>
formula	FeCl <sub>6</sub> O <sub>4</sub> N <sub>6</sub> C <sub>47</sub> H <sub>53</sub>	FeCl <sub>2</sub> O <sub>4</sub> N <sub>3</sub> C <sub>41</sub> H <sub>48</sub>
fw	1034.5	801.6
space group	<i>Pbca</i>	<i>C2/c</i>
temp, K	292 ± 1	292 ± 1
<i>a</i> , Å	26.171 (6)	18.754 (12)
<i>b</i> , Å	38.014 (8)	16.160 (9)
<i>c</i> , Å	10.020 (2)	27.350 (15)
β, deg		103.97 (4)
<i>V</i> , Å <sup>3</sup>	9968.5	8043.7
<i>Z</i>	8	8
<i>d</i> <sub>calcd</sub> , g/cm <sup>3</sup>	1.379	1.324
<i>d</i> <sub>obsd</sub> , g/cm <sup>3</sup>	1.37	1.31
radiation	graphite-monochromated Mo Kα (λ = 0.71073 Å)	
scan technique		θ-2θ
cryst dimens, mm	0.30 × 0.50 × 0.64	0.75 × 0.75 × 0.10
scan range, deg	0.30 in ω	0.75 below Kα <sub>1</sub> to 0.75 above Kα <sub>2</sub>
scan rate, deg/min		2-12
bkgd	0.5 times scan at the extremes of scan	
2θ limits, deg		3.5-54.90
no. of unique measd data	11 609	9216
criterion for observn		<i>F</i> <sub>0</sub> > 3σ( <i>F</i> <sub>0</sub> )
unique obsd data	4593	4800
data/parameter	8.0	9.4
μ, mm <sup>-1</sup>	0.67	0.55
<i>R</i> <sub>1</sub>	0.092	0.093
<i>R</i> <sub>2</sub>	0.095	0.101
goodness of fit	2.17	2.68

material was isolated. These results were repeated several times; furthermore, subsequent crystallization experiments employing a 4/5 3-Cl-py/[Fe(OEP)(OCIO<sub>3</sub>)] ratio gave results that were indistinguishable from the above. Crystals of both complexes were very similar in their external appearance; each appeared to be monoclinic rhombs. *Caution!* Although we have experienced no difficulties with these compounds, perchlorate salts are potentially hazardous owing to the possibility of unexpected detonations. The use of small quantities of material is advised.

A pure sample of the five-coordinate complex, free of the six-coordinate contaminant, was achieved by differential flotation. A mixture of crystals of the two species was added to a mixture of heptane and carbon tetrachloride and the density of the solution carefully adjusted to 1.334 g/cm<sup>3</sup>. The material that sank to the bottom was rejected; the material that floated was retained as the purest sample of [Fe(OEP)(3-Cl-py)]ClO<sub>4</sub> obtainable for physical measurements. Mössbauer spectra were obtained on unenriched material by using procedures described previously.<sup>16</sup> The spectra<sup>17</sup> showed a single component, confirming the efficacy of the flotation procedure for purification.

**Structural Characterizations.** Both crystalline compounds were examined on a Nicolet P1 diffractometer. Least-squares refinement of the setting angles of 60 reflections, collected at ±2θ, gave the cell constants reported in Table I. All measurements utilized graphite-monochromated Mo Kα radiation (λ = 0.71073 Å) at the ambient laboratory temperature of 19 ± 1 °C. Data for [Fe(OEP)(3-Cl-py)]ClO<sub>4</sub> were collected with use of θ-2θ scans and Mo Kα radiation and that for [Fe(OEP)(3-Cl-py)<sub>2</sub>]ClO<sub>4</sub> with use of ω scans. Complete details of the intensity collection parameters and refinements are summarized in Table I.

The structures of both complexes were determined by using the direct-methods program MULTAN<sup>78</sup>.<sup>18</sup> Standard values for the atomic

**Table II.** Fractional Coordinates for [Fe(OEP)(3-Cl-py)]ClO<sub>4</sub><sup>a</sup>

Atom	x	y	z
Fe	0.55366 (5)	0.15082 (5)	0.67203 (3)
Cl (1)	0.86144 (13)	0.10793 (17)	0.72803 (9)
Cl (2)	0.42650 (14)	-0.29651 (14)	0.54977 (8)
N (1)	0.52988 (27)	0.2650 (3)	0.64709 (17)
N (2)	0.49387 (26)	0.1088 (3)	0.60730 (17)
N (3)	0.56052 (26)	0.0375 (3)	0.70000 (17)
N (4)	0.59066 (28)	0.1933 (3)	0.74171 (18)
N (5)	0.6574 (3)	0.1513 (3)	0.65346 (19)
C (a1)	0.5503 (4)	0.3383 (4)	0.67393 (25)
C (a2)	0.5003 (4)	0.2899 (4)	0.59856 (23)
C (a3)	0.4662 (3)	0.1525 (4)	0.56378 (22)
C (a4)	0.4763 (3)	0.0264 (4)	0.59418 (23)
C (a5)	0.5388 (3)	-0.0359 (4)	0.67386 (24)
C (a6)	0.5963 (3)	0.0113 (4)	0.74783 (25)
C (a7)	0.6181 (3)	0.1497 (5)	0.78506 (22)
C (a8)	0.5992 (4)	0.2768 (5)	0.75644 (23)
C (b1)	0.5343 (4)	0.4081 (4)	0.63949 (28)
C (b2)	0.5020 (4)	0.3787 (4)	0.59300 (26)
C (b3)	0.4288 (4)	0.1000 (4)	0.52369 (22)
C (b4)	0.4318 (4)	0.0219 (4)	0.54278 (24)
C (b5)	0.5637 (4)	-0.1066 (4)	0.70683 (26)
C (b6)	0.5993 (4)	-0.0769 (4)	0.75155 (25)
C (b7)	0.6451 (4)	0.2035 (5)	0.82698 (23)
C (b8)	0.6341 (4)	0.2821 (5)	0.80951 (24)
C (m1)	0.5826 (4)	0.3433 (4)	0.72419 (24)
C (m2)	0.4710 (4)	0.2372 (4)	0.55983 (22)
C (m3)	0.4981 (3)	-0.0398 (4)	0.62562 (23)
C (m4)	0.6216 (4)	0.0655 (5)	0.78732 (23)
C (11)	0.5696 (8)	0.5036 (7)	0.6523 (4)
C (12)	0.5110 (9)	0.5279 (9)	0.6685 (5)
C (21)	0.4740 (5)	0.4265 (4)	0.54582 (26)
C (22)	0.3910 (6)	0.4325 (5)	0.5310 (3)
C (31)	0.3876 (4)	0.1276 (4)	0.47277 (24)
C (32)	0.3135 (5)	0.1596 (6)	0.4723 (3)
C (41)	0.3962 (4)	-0.0555 (4)	0.51822 (26)
C (42)	0.3222 (6)	-0.0699 (6)	0.5313 (4)
C (51)	0.5482 (4)	-0.1955 (5)	0.69090 (29)
C (52)	0.6032 (5)	-0.2294 (5)	0.6669 (3)
C (61)	0.6387 (4)	-0.1236 (5)	0.79709 (27)
C (62)	0.7201 (5)	-0.1264 (5)	0.8031 (3)
C (71)	0.6813 (4)	0.1752 (5)	0.87943 (23)
C (72)	0.7591 (4)	0.1470 (5)	0.88576 (27)
C (81)	0.6509 (5)	0.3619 (5)	0.83782 (26)
C (82)	0.7205 (6)	0.4006 (5)	0.8350 (3)
C (1)	0.6659 (4)	0.1797 (5)	0.60981 (29)
C (2)	0.7335 (5)	0.1869 (6)	0.5975 (3)
C (3)	0.7961 (5)	0.1633 (6)	0.6352 (3)
C (4)	0.7865 (4)	0.1347 (4)	0.68048 (27)
C (5)	0.7177 (4)	0.1294 (4)	0.68840 (25)
O (1)	0.3705 (21)	-0.2963 (22)	0.5080 (11)
O (2)	0.3909 (21)	-0.2491 (23)	0.5798 (15)
O (3)	0.4275 (20)	-0.3701 (17)	0.5701 (16)
O (4)	0.4939 (17)	-0.2635 (17)	0.5513 (11)
O (5)	0.4036 (13)	-0.2647 (11)	0.5014 (7)
O (6)	0.4225 (16)	-0.2397 (14)	0.5877 (9)
O (7)	0.3855 (19)	-0.3677 (18)	0.5527 (13)
O (8)	0.5039 (13)	-0.3271 (14)	0.5577 (7)

<sup>a</sup>The estimated standard deviations of the least significant digits are given in parentheses.

scattering factors including corrections for anomalous dispersion were employed in the structure analyses. Structure analysis was straightforward<sup>19</sup> except for a disordered perchlorate in [Fe(OEP)(3-Cl-py)]ClO<sub>4</sub>. The perchlorate oxygen atoms were disordered around a common (or nearly so) chlorine atom center. Each of the eight oxygen positions was assigned an occupancy factor of 0.5. Difference Fourier syntheses led to the location of all hydrogen atoms in both complexes. The hydrogen

(16) Mashiko, T.; Kastner, M. E.; Spartalian, K.; Scheidt, W. R.; Reed, C. A. *J. Am. Chem. Soc.* **1978**, *100*, 6354-6362.

(17) Gupta, G. P.; Lang, G.; Scheidt, W. R.; Geiger, D. K.; Reed, C. A. *J. Chem. Phys.* **1986**, *25*, 5212-5220.

(18) Programs used in this study included local modifications of Main, Hull, Lessinger, Germain, Declercq, and Woolfson's MULTAN<sup>78</sup>, Jacobson's ALLS, Zalkin's FORDAP, Busing and Levy's ORFFE and ORFLS, and Johnson's ORTEP2. Atomic form factors were from: Cromer, D. T.; Mann, J. B. *Acta Crystallogr., Sect. A: Cryst. Phys., Diffr., Theor. Gen. Crystallogr.* **1968**, *A24*, 321-323. Real and imaginary corrections for anomalous dispersion in the form factor of the iron and chlorine atoms were from: Cromer, D. T.; Liberman, D. J. *J. Chem. Phys.* **1970**, *53*, 1891-1898. Scattering factors for hydrogen were from: Stewart, R. F.; Davidson, E. R.; Simpson, W. T. *J. Chem. Phys.* **1965**, *42*, 3175-3187. All calculations were performed on a VAX 11/730 computer.

(19) A reviewer has asked about our choice of the centrosymmetric space group *C2/c* rather than the noncentrosymmetric alternative. In this analysis, we assumed the centrosymmetric choice of space group. All subsequent developments during structure analysis were consistent with this choice, and we believe that we have made the correct choice. In other similar problems, we have explored both centro- and noncentrosymmetric space group choices. In no case have we ever been able to judge that the noncentrosymmetric choice was the better one on the basis of refinement behavior or internal self-consistency of the bond parameters.

Table III. Fractional Coordinates for  $[\text{Fe}(\text{OEP})(3\text{-Cl-py})_2]\text{ClO}_4^a$ 

Atom	x	y	z
Fe	0.63372(4)	0.615083(27)	0.24504(12)
C1(1)	0.63851(13)	0.55669(7)	0.78377(25)
C1(2)	0.63638(14)	0.67322(8)	-0.29578(26)
C1(3)	0.61057(9)	0.40016(6)	0.25966(29)
C1(4)	0.11240(17)	0.22008(12)	-0.0812(5)
C1(5)	0.04482(15)	0.18299(12)	0.0897(5)
C1(6)	0.15449(15)	0.17455(13)	0.1115(4)
N(1)	0.59445(25)	0.65573(17)	0.3239(6)
N(2)	0.57589(25)	0.58296(17)	0.2912(6)
N(3)	0.67241(24)	0.57450(17)	0.1662(6)
N(4)	0.69062(24)	0.64782(17)	0.1967(6)
N(5)	0.67188(27)	0.60495(18)	0.4460(6)
N(6)	0.59764(28)	0.62543(18)	0.0365(7)
C(a1)	0.6113(4)	0.69027(23)	0.3301(8)
C(a2)	0.5441(4)	0.65485(25)	0.3734(8)
C(a3)	0.5272(3)	0.59188(22)	0.3411(8)
C(a4)	0.5730(3)	0.54703(23)	0.2654(9)
C(a5)	0.6585(3)	0.53956(22)	0.1630(8)
C(a6)	0.7199(3)	0.57528(22)	0.1054(8)
C(a7)	0.7346(3)	0.63897(22)	0.1272(8)
C(a8)	0.6941(3)	0.68336(23)	0.2251(7)
C(b1)	0.5695(5)	0.71142(24)	0.3872(10)
C(b2)	0.5294(4)	0.69002(27)	0.4107(10)
C(b3)	0.4955(4)	0.56225(27)	0.3434(10)
C(b4)	0.5210(4)	0.53552(27)	0.2997(11)
C(b5)	0.6967(3)	0.51866(23)	0.1025(9)
C(b6)	0.7339(3)	0.54038(23)	0.0633(9)
C(b7)	0.7666(3)	0.67038(25)	0.1097(8)
C(b8)	0.7406(4)	0.69690(24)	0.1737(8)
C(m1)	0.6593(4)	0.70221(22)	0.2877(8)
C(m2)	0.5157(3)	0.62487(26)	0.3822(9)
C(m3)	0.6129(4)	0.52739(21)	0.2103(9)
C(m4)	0.7472(3)	0.60578(23)	0.0856(8)
C(1)	0.6483(3)	0.58664(22)	0.5430(9)
C(2)	0.6704(4)	0.58070(25)	0.6643(10)
C(3)	0.7163(5)	0.59260(27)	0.6906(9)
C(4)	0.7417(4)	0.6108(3)	0.5935(11)
C(5)	0.7181(4)	0.61688(26)	0.4715(9)
C(6)	0.6233(3)	0.64396(22)	-0.0550(9)
C(7)	0.6028(5)	0.64940(27)	-0.1804(10)
C(8)	0.5549(6)	0.6342(4)	-0.2131(11)
C(9)	0.5294(4)	0.6159(4)	-0.1183(13)
C(10)	0.5515(4)	0.61178(27)	0.0060(10)
C(11)	0.5697(5)	0.7517(3)	0.3985(12)
C(12)	0.5845(6)	0.7627(3)	0.5255(14)
C(21)	0.4736(5)	0.7004(3)	0.4556(14)
C(22)	0.4740(5)	0.7019(4)	0.5990(18)
C(31)	0.4405(4)	0.5639(3)	0.3800(15)
C(32)	0.4074(5)	0.5828(4)	0.2782(18)
C(41)	0.5042(9)	0.4938(8)	0.3120(24)
C(42)	0.4941(8)	0.4919(4)	0.1942(27)
C(51)	0.6934(4)	0.47983(26)	0.0838(10)
C(52)	0.6700(6)	0.46854(29)	-0.0405(15)
C(61)	0.7825(5)	0.5306(3)	-0.0179(14)
C(62)	0.8179(5)	0.5129(4)	0.0425(20)
C(71)	0.8156(3)	0.67161(24)	0.0340(9)
C(72)	0.8082(4)	0.68038(29)	-0.1111(11)
C(81)	0.7588(4)	0.73495(25)	0.1864(9)
C(82)	0.7376(5)	0.75952(26)	0.0826(12)
O(1)	0.6559(3)	0.40405(23)	0.3278(10)
O(2)	0.5769(3)	0.37758(22)	0.3133(9)
O(3)	0.5881(3)	0.43208(21)	0.2406(11)
O(4)	0.6273(4)	0.38555(26)	0.1392(11)
C(ch)	0.1033(4)	0.18055(29)	0.0069(11)

<sup>a</sup> The estimated standard deviations of the least significant digits are given in parentheses.

atom positions were idealized ( $C-H = 0.95 \text{ \AA}$ ,  $B(H) = B(C) + 1.0 \text{ \AA}^2$ ) and were included in all subsequent refinement cycles as fixed contributors with additional reidealization as required. Both structures were refined to convergence with anisotropic temperature factors for all heavy atoms. The thermal parameters of one ethyl group in each compound were observed to be larger than normal, suggesting positional disorder, which is commonly found for octaethylporphyrin derivatives. However, attempts to find a two-position model from difference Fourier maps were unsuccessful. Final difference Fourier syntheses for both were judged essentially featureless. Final atomic coordinates are listed in Tables II and III for  $[\text{Fe}(\text{OEP})(3\text{-Cl-py})]\text{ClO}_4$  and  $[\text{Fe}(\text{OEP})(3\text{-Cl-py})_2]\text{ClO}_4$ ,

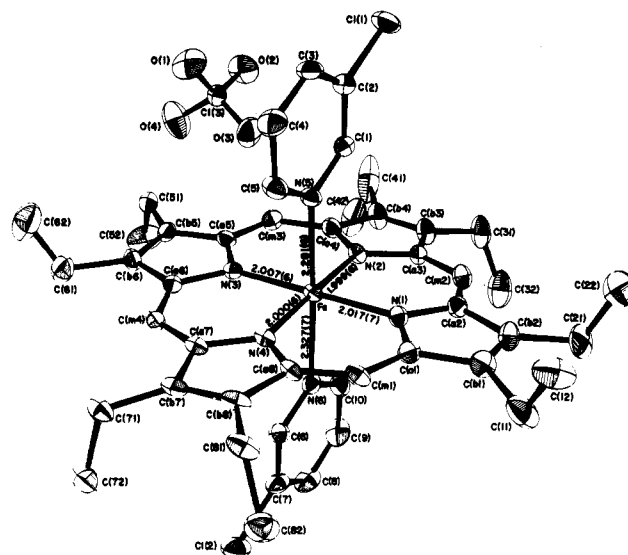


Figure 1. ORTEP plot of the molecular structure of  $[\text{Fe}(\text{OEP})(3\text{-Cl-py})_2]\text{ClO}_4$  as it exists in the crystal. The atom-labeling scheme is displayed as well as the bond distances in the coordination group of the molecule. Atoms are contoured at the 50% probability level.

respectively. Final anisotropic temperature factors and fixed hydrogen atom positions are given in Tables IS-IVS of the supplementary material.

## Results and Discussion

The observation that two kinds of crystals (and molecules) arise from the reaction of equimolar quantities of 3-chloropyridine and  $[\text{Fe}(\text{OEP})(\text{OClO}_3)]$  is the result of the examination of a rather large number of crystals in order to obtain one crystal of adequate quality to collect intensity data. In the course of this study a new cell, that of  $[\text{Fe}(\text{OEP})(3\text{-Cl-py})_2]\text{ClO}_4$ , in addition to that of  $[\text{Fe}(\text{OEP})(3\text{-Cl-py})]\text{ClO}_4$  was observed. The new unit cell constants and cell volume suggested that a species with stoichiometry different from that of crystalline  $[\text{Fe}(\text{OEP})(3\text{-Cl-py})]\text{ClO}_4$  was the cause of this second cell. In retrospect, crystals of the two species may have been distinguishable on the basis of crystal morphology, but the differences are not sufficient to allow complete confidence in the sorting. The fraction of isolated crystalline material that is six-coordinate cannot be estimated with complete precision, but it is clearly a minor species. We estimate<sup>20</sup> that 10–20% of the isolated crystalline material is  $[\text{Fe}(\text{OEP})(3\text{-Cl-py})_2]\text{ClO}_4$ . It should be noted that even when  $[\text{Fe}(\text{OEP})(\text{OClO}_3)]$  is present in 20% excess, some six-coordinate species is formed. (The presence of  $[\text{Fe}(\text{OEP})(3\text{-Cl-py})_2]\text{ClO}_4$  in each preparation was always confirmed by determination of unit cell constants by X-ray diffraction; at least one crystal having the cell constants of  $[\text{Fe}(\text{OEP})(3\text{-Cl-py})_2]\text{ClO}_4$  was found in each preparation.) Physical separation by flotation does appear to provide a means of isolating the pure five-coordinate material for physical characterization. These results demonstrate that it can be quite difficult to correctly assign the nature and number of axial ligands in the absence of complete characterization.

The present crystalline phase of  $[\text{Fe}(\text{OEP})(3\text{-Cl-py})_2]\text{ClO}_4$  is the third such phase we have characterized.<sup>10,11</sup> As noted in the introduction, one phase is an admixed intermediate-spin state,<sup>11</sup> this species is most directly comparable to the current crystalline phase. Figure 1 illustrates the molecular structure of the present phase. Except for the orientation of the peripheral ethyl groups, the molecule has a near inversion center at the iron atom. As can be seen from Figure 1, the two pyridine rings are essentially coplanar (dihedral angle between the two planes is  $3.8^\circ$ ). Further, the two pyridine rings nearly eclipse the complexing equatorial  $\text{Fe}-\text{N}_p$  bonds; the observed angles are  $8.7$  and  $6.1^\circ$ . The significance of this type of ligand orientation and its relationship to

(20) This estimate is based on two assumptions: (i) all of the 3-chloropyridine reacts to form a complex and (ii) the amorphous (or microcrystalline) material is the starting perchlorato complex.

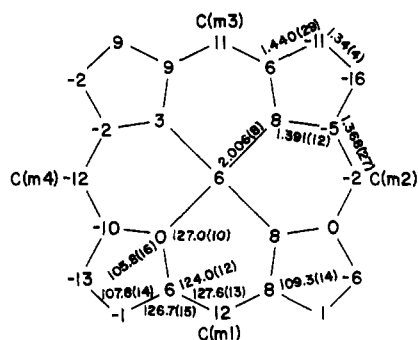


**Figure 2.** Formal diagram of the porphinato core in  $[\text{Fe}(\text{OEP})(3\text{-Cl-py})_2]\text{ClO}_4$  displaying the deviation of each atom (in units of 0.01 Å) from the mean plane of the porphinato core. The small iron atom displacement is toward the N(5) pyridine ligand. Typical uncertainties in the displacements are 0.005–0.007 Å. Averaged values of bond parameters are also displayed.

**Table IV.** Bond Lengths (Å) in  $[\text{Fe}(\text{OEP})(3\text{-Cl-Py})_2]\text{ClO}_4 \cdot \text{CHCl}_3^a$

Fe–N(1)	2.017 (7)	C(b5)–C(b6)	1.336 (11)
Fe–N(2)	1.999 (6)	C(b7)–C(b8)	1.375 (11)
Fe–N(3)	2.007 (6)	C(1)–C(2)	1.366 (11)
Fe–N(4)	2.000 (6)	C(2)–C(3)	1.309 (12)
Fe–N(5)	2.281 (6)	C(2)–Cl(1)	1.722 (10)
Fe–N(6)	2.327 (7)	C(3)–C(4)	1.366 (13)
N(1)–C(a1)	1.386 (10)	C(4)–C(5)	1.389 (12)
N(1)–C(a2)	1.409 (10)	C(6)–C(7)	1.381 (12)
N(2)–C(a3)	1.409 (9)	C(7)–C(8)	1.418 (5)
N(2)–C(a4)	1.392 (9)	C(7)–Cl(2)	1.711 (11)
N(3)–C(a5)	1.377 (9)	C(8)–C(9)	1.354 (15)
N(3)–C(a6)	1.384 (9)	C(9)–C(10)	1.383 (13)
N(4)–C(a7)	1.386 (9)	C(11)–C(b1)	1.537 (14)
N(4)–C(a8)	1.383 (9)	C(11)–C(12)	1.394 (15)
N(5)–C(1)	1.345 (9)	C(21)–C(b2)	1.578 (15)
N(5)–C(5)	1.316 (10)	C(21)–C(22)	1.438 (18)
N(6)–C(6)	1.337 (10)	C(31)–C(b3)	1.487 (13)
N(6)–C(10)	1.349 (10)	C(31)–C(32)	1.519 (18)
C(a1)–C(b1)	1.473 (12)	C(41)–C(b4)	1.650 (29)
C(a1)–C(m1)	1.403 (11)	C(41)–C(42)	1.21 (3)
C(a2)–C(b2)	1.440 (12)	C(21)–C(b5)	1.490 (11)
C(a2)–C(m2)	1.363 (11)	C(51)–C(52)	1.453 (14)
C(a3)–C(b3)	1.399 (11)	C(61)–C(b6)	1.555 (13)
C(a3)–C(m2)	1.354 (11)	C(61)–C(62)	1.296 (16)
C(a4)–C(b4)	1.470 (11)	C(71)–C(b7)	1.490 (12)
C(a4)–C(m3)	1.398 (11)	C(71)–C(72)	1.504 (13)
C(a5)–C(b5)	1.412 (11)	C(81)–C(b8)	1.528 (11)
C(a5)–C(m3)	1.365 (11)	C(81)–C(82)	1.504 (13)
C(a6)–C(b6)	1.440 (10)	Cl(3)–O(1)	1.376 (7)
C(a6)–C(m4)	1.376 (10)	Cl(3)–O(2)	1.343 (7)
C(a7)–C(b7)	1.470 (10)	Cl(3)–O(3)	1.362 (7)
C(a7)–C(m4)	1.369 (10)	Cl(3)–O(4)	1.399 (9)
C(a8)–C(b8)	1.418 (11)	C(ch)–Cl(4)	1.759 (11)
C(a8)–C(m1)	1.317 (11)	C(ch)–Cl(5)	1.744 (11)
C(b1)–C(b2)	1.348 (12)	C(ch)–Cl(6)	1.716 (11)
C(b3)–C(b4)	1.292 (12)		

<sup>a</sup> The numbers in parentheses are the estimated standard deviations.

the spin state of the iron(III) atom have been previously discussed.<sup>11</sup> Both pyridine ligands are nearly perpendicular to the mean porphinato plane. Figure 2 illustrates the porphinato core conformation. The deviation from exact planarity is unremarkable.

Individual values of bond distances and angles are tabulated in Tables IV and V. The averaged values for the various chemical classes in the porphinato core are displayed in Figure 2. The bond distances shown in Figure 2 are the structural signature of an admixed intermediate-spin state for the iron(III) atom. The average value of the Fe–N<sub>p</sub> bond distances is 2.006 (8) Å.<sup>21</sup> The axial bond distances are quite long at 2.281 (6) and 2.327 (7) Å

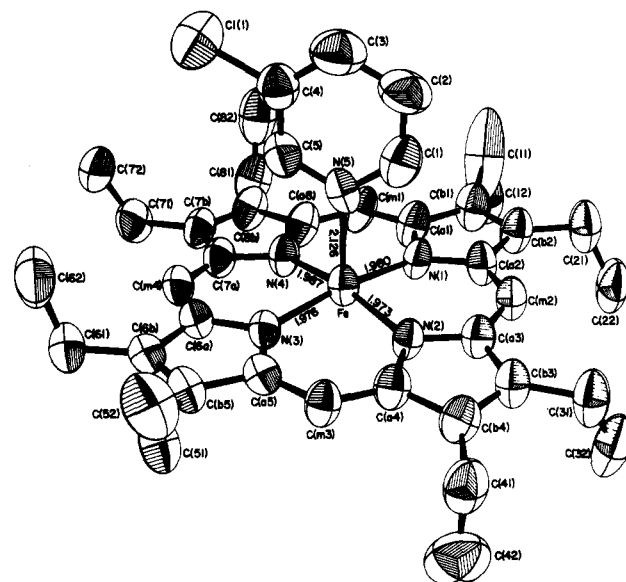


**Figure 3.** ORTEP plot of the molecular structure of  $[\text{Fe}(\text{OEP})(3\text{-Cl-py})_2]\text{ClO}_4$  as it exists in the crystal. The same information as shown in Figure 1 is given.

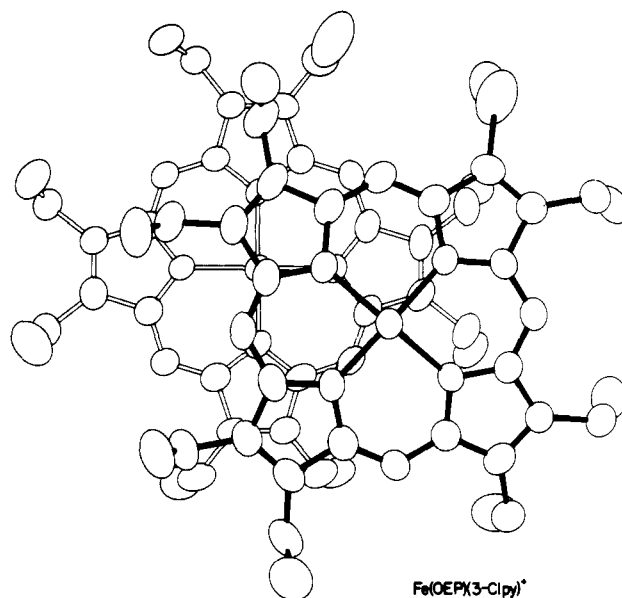


**Figure 4.** Computer-drawn model of the two  $[\text{Fe}(\text{OEP})(3\text{-Cl-py})]^+$  ions related by the twofold axis, showing the overlap of the two cores. The lower porphinato core (open bonds) is in the plane of the paper, and the upper core is drawn with solid bonds.

(average 2.304 Å). These values can be compared with the previously<sup>11,22</sup> characterized monoclinic phase of  $[\text{Fe}(\text{OEP})(3\text{-Cl-py})_2]\text{ClO}_4$  in which an average Fe–N<sub>p</sub> distance of 2.005 (6) Å and an average axial distance of 2.310 (17) Å were found. Given the close convergence of these parameters and the distinct structural patterns<sup>6</sup> for the three possible spin states, we conclude that the electronic state of this third crystalline form is definitely an admixed  $S = 3/2$  state.

As was noted in the previous characterization of the monoclinic<sup>11</sup> intermediate-spin form of  $[\text{Fe}(\text{OEP})(3\text{-Cl-py})_2]\text{ClO}_4$ , the relative orientation of the axial ligand planes is thought to be a significant factor leading to the observed  $S = 3/2$  state. It was suggested that the orientation of the two axial pyridines with a small  $\phi$  value<sup>23</sup>

(21) The numbers in parentheses following this and all other averaged bond distances are the estimated standard deviations calculated on the assumption that the averaged values are drawn from the same population.

(22) Extensive physical characterization of this phase led to the conclusive assignment of an admixed intermediate-spin state.

(23)  $\phi$  is defined as the dihedral angle between the pyridine plane and the coordinate plane containing the metal and two opposite porphinato nitrogen atoms.

Table V. Bond Angles (deg) in  $[\text{Fe}(\text{OEP})(3\text{-Cl-py})_2]\text{ClO}_4 \cdot \text{CHCl}_3^a$ 

N(1)FeN(2)	89.50 (28)	C(a5)C(b5)C(51)	124.8 (8)
N(1)FeN(3)	179.66 (27)	C(b6)C(b5)C(51)	128.1 (8)
N(1)FeN(4)	89.86 (27)	C(a6)C(b6)C(b5)	107.3 (8)
N(1)FeN(5)	90.37 (25)	C(a6)C(b6)C(61)	125.6 (8)
N(1)FeN(6)	90.89 (24)	C(b5)C(b6)C(61)	127.1 (9)
N(2)FeN(3)	90.2 (27)	C(a7)C(b7)C(b8)	104.9 (8)
N(2)FeN(4)	178.85 (26)	C(a7)C(b7)C(71)	125.2 (9)
N(2)FeN(5)	91.36 (26)	C(b8)C(b7)C(71)	129.8 (9)
N(2)FeN(6)	90.23 (27)	C(a8)C(b8)C(b7)	109.2 (8)
N(3)FeN(4)	90.43 (27)	C(a8)C(b8)C(81)	125.5 (9)
N(3)FeN(5)	89.81 (24)	C(b7)C(b8)C(81)	125.3 (9)
N(3)FeN(6)	88.93 (23)	C(a1)C(m1)C(a8)	126.0 (8)
N(4)FeN(5)	89.59 (25)	C(a2)C(m2)C(a3)	129.2 (8)
N(4)FeN(6)	88.82 (26)	C(a4)C(m3)C(a5)	127.6 (8)
N(5)FeN(6)	177.97 (26)	C(a6)C(m4)C(a7)	127.4 (8)
C(a1)N(1)C(a2)	107.7 (7)	N(5)C(1)C(2)	122.2 (8)
C(a3)N(2)C(a4)	104.6 (7)	C(1)C(2)C(3)	120.7 (9)
C(a5)N(3)C(a6)	104.3 (7)	C(1)C(2)Cl(1)	120.0 (8)
C(a7)N(4)C(a8)	106.6 (7)	C(3)C(2)Cl(1)	119.2 (9)
C(1)N(5)C(5)	117.4 (7)	C(2)C(3)C(4)	118.5 (10)
C(6)N(6)C(10)	119.7 (8)	C(3)C(4)C(5)	119.7 (10)
C(1)C(a1)C(b1)	107.4 (8)	C(4)C(5)N(5)	121.4 (9)
N(1)C(a1)C(m1)	125.3 (8)	N(6)C(6)C(7)	120.6 (9)
C(b1)C(a1)C(m1)	127.3 (9)	C(6)C(7)C(8)	119.4 (10)
N(1)C(a2)C(b2)	108.5 (8)	C(6)C(7)Cl(2)	119.6 (10)
N(1)C(a2)C(m2)	123.6 (8)	C(8)C(7)Cl(2)	120.9 (9)
C(b2)C(a2)em2	127.9 (6)	C(7)C(8)C(9)	118.9 (10)
N(2)C(a3)C(b3)	110.4 (7)	C(8)C(9)C(10)	118.9 (11)
N(2)C(a3)C(m2)	122.2 (8)	N(6)C(10)C(9)	122.4 (10)
C(b3)C(a3)C(m2)	127.4 (8)	C(b1)C(11)C(12)	111.5 (11)
N(2)C(a4)C(b4)	107.4 (8)	C(b2)C(21)C(22)	106.8 (12)
N(2)C(a4)C(m3)	123.8 (8)	C(23)C(31)C(32)	113.9 (11)
C(b4)C(a4)C(m3)	128.7 (9)	C(b4)C(41)C(42)	92.5 (25)
N(3)C(a5)C(b5)	111.5 (8)	C(b5)C(51)C(52)	115.1 (9)
N(3)C(a5)C(m3)	123.3 (8)	C(b6)C(61)C(62)	117.7 (13)
C(b5)C(a5)C(m3)	125.2 (8)	C(b7)C(71)C(72)	112.9 (8)
N(3)C(a6)C(b6)	109.8 (7)	C(b8)C(81)C(82)	114.5 (8)
N(3)C(a6)C(m4)	123.2 (8)	Fe(1)C(a1)	125.5 (6)
C(b6)C(a6)C(m4)	127.0 (8)	FeN(1)C(a2)	126.6 (6)
N(4)C(a7)C(b7)	109.6 (8)	FeN(2)C(a3)	128.3 (6)
N(4)C(a7)C(m4)	125.2 (7)	FeN(2)C(a4)	126.7 (6)
C(b7)C(a7)C(m4)	125.1 (8)	FeN(3)C(a5)	128.1 (6)
N(4)C(a8)C(b8)	109.6 (8)	FeN(3)C(a6)	127.6 (5)
N(4)C(a8)C(m1)	125.7 (8)	FeN(4)C(a7)	126.0 (5)
C(b8)C(a8)C(m1)	124.6 (8)	FeN(4)C(a8)	127.4 (6)
C(a1)C(b1)C(b2)	108.4 (8)	FeN(5)C(1)	121.6 (6)
C(a1)C(b1)C(11)	124.8 (10)	FeN(5)C(5)	121.0 (6)
C(b2)C(b1)C(11)	126.3 (10)	FeN(6)C(6)	120.1 (6)
C(a2)C(b2)C(b1)	108.0 (9)	FeN(6)C(10)	120.1 (6)
C(a2)C(b2)C(21)	123.4 (10)	O(1)Cl(3)O(2)	115.8 (6)
C(b1)C(b2)C(21)	128.3 (10)	O(1)Cl(3)O(3)	110.2 (6)
C(a3)C(b3)C(b4)	108.8 (8)	O(1)Cl(3)O(4)	101.6 (6)
C(a3)C(b3)C(31)	123.0 (9)	O(2)Cl(3)O(3)	110.0 (6)
C(b4)C(b3)C(31)	128.0 (9)	O(2)Cl(3)O(4)	107.3 (6)
C(a4)C(b4)C(b3)	108.8 (8)	O(3)Cl(3)O(4)	111.6 (7)
C(a4)C(b4)C(41)	123.4 (2)	Cl(4)C(ch)Cl(5)	108.2 (6)
C(b3)C(b4)C(41)	126.4 (11)	Cl(4)C(ch)Cl(6)	108.4 (6)
C(a5)C(b5)C(b6)	107.1 (8)	Cl(5)C(ch)Cl(6)	113.7 (6)

<sup>a</sup>The numbers in parentheses are the estimated standard deviations.

required either a high-spin or admixed intermediate-spin state. The current observations endorse this suggestion. As in the earlier case, the specific ligand orientations appear locked in place by crystal-packing interactions. The reason for the eclipsed orientation of the pyridine rings is not known with certainty, but recent theoretical calculations<sup>24</sup> do suggest an electronic basis in both five- and six-coordinate imidazole complexes.

The molecular structure of the major synthetic target of this investigation is shown in Figure 3. From our previous investigation of five-coordinate  $[\text{Fe}(\text{OEP})(2\text{-MeHIm})]\text{ClO}_4$ ,<sup>4</sup> we had expected that a stabilizing porphyrin  $\pi$ - $\pi$  interaction between two  $[\text{Fe}(\text{OEP})(3\text{-Cl-py})]^+$  ions would be found. This is indeed the case.

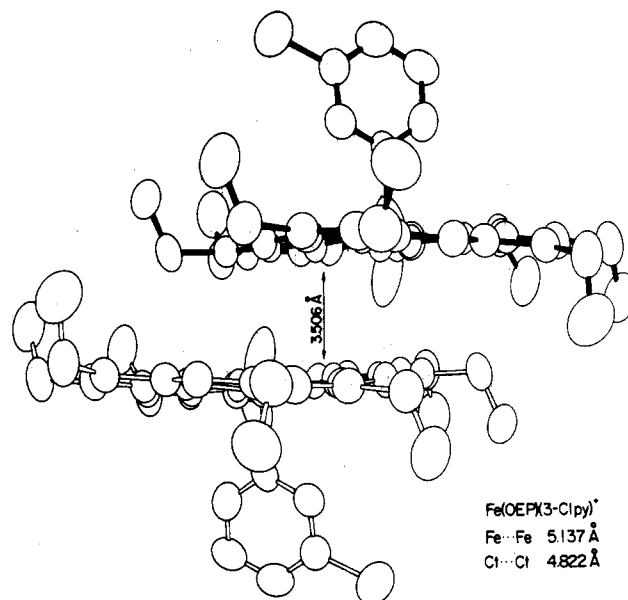


Figure 5. Second view of the  $\pi$ - $\pi$  dimer. The planes of the cores are perpendicular to the plane of the paper. The two cores are drawn with the same open and filled bonds as in Figure 4.

The interactions in  $[\text{Fe}(\text{OEP})(3\text{-Cl-py})]\text{ClO}_4$  are shown in Figures 4 and 5. Figure 4 is a view perpendicular to the porphyrato planes that shows the "slipped" nature of the  $\pi$ - $\pi$  complex. Figure 5, a view  $90^\circ$  from that of Figure 4, shows the separation between the two porphyrato planes. The two planes are related by a twofold symmetry operation and are not quite parallel; the dihedral angle is  $4.6^\circ$ . The separation between the two planes is 3.506 Å, the Fe...Fe distance is 5.137 Å, and the Cl...Cl distance is 4.822 Å. These separations are much larger than those found in the two crystalline forms of  $[\text{Fe}(\text{OEP})(2\text{-MeHIm})]\text{ClO}_4$ . The interplanar spacings are 3.312 and 3.42 Å, and Fe...Fe distances are 4.280 and 4.60 Å, and the Cl...Cl distances are 3.635 and 4.04 Å for the methylene bromide and chloroform solvated forms, respectively. The differences in the solid-state intermolecular separations suggest that the  $\pi$ - $\pi$  interaction is somewhat weaker in the present case. This could explain why some six-coordination is observed with 3-chloropyridine but not with 2-methylimidazole under equimolar reaction conditions. Such  $\pi$ - $\pi$  differences might persist in solution, leading to a smaller relative value of  $K_2$  for the reaction with 2-methylimidazole. Thus the formation of some six-coordinate  $[\text{Fe}(\text{OEP})(3\text{-Cl-py})_2]\text{ClO}_4$  could be expected, but much less six-coordinate  $[\text{Fe}(\text{OEP})(2\text{-MeHIm})_2]\text{ClO}_4$ , a known<sup>25</sup> species, would be formed under the same reaction conditions.

The distinction in the apparent strength of the  $\pi$ - $\pi$  interaction is also reflected in the magnetic properties. The  $\pi$ - $\pi$  interaction gives rise to an antiferromagnetic interaction between ferric ions. In high-spin  $[\text{Fe}(\text{OEP})(2\text{-MeHIm})]^+$ ,<sup>26</sup> a detailed analysis of the magnetic susceptibility and Mössbauer spectra gave an exchange interaction of about  $-0.8 \text{ cm}^{-1}$ . The exchange interaction that best fits the data for  $[\text{Fe}(\text{OEP})(3\text{-Cl-py})]\text{ClO}_4$  is smaller ( $-0.6 \text{ cm}^{-1}$ ).<sup>17</sup> This more weakly modulated interaction of the metal ions is consistent with a larger interplanar separation in the  $\pi$ - $\pi$  structure. A complete analysis of the susceptibility data and Mössbauer spectra (1.54–128 K and 0–6 T applied magnetic field) have been published elsewhere.<sup>17</sup> The magnetic susceptibility data have been analyzed in terms of a "Maltempo model"<sup>27</sup> modified by inclusion of the antiferromagnetic exchange interaction between neighboring ions in the dimer structure. Values of the Mössbauer chemical shift,  $\delta = 0.36 \text{ mm/s}$  (relative to metallic iron), and the temperature-independent quadrupole splitting,  $\Delta E = 3.23 \text{ mm/s}$ ,

(25) Geiger, D. K.; Lee, Y. J.; Scheidt, W. R. *J. Am. Chem. Soc.* **1984**, *106*, 6339–6343.

(26) Gupta, G. P.; Lang, G.; Scheidt, W. R.; Geiger, D. K.; Reed, C. A. *J. Chem. Phys.* **1985**, *83*, 5945–5952.

(27) Maltempo, M. M. *J. Chem. Phys.* **1974**, *61*, 2540–2547.

(24) Scheidt, W. R.; Chipman, D. M. *J. Am. Chem. Soc.* **1986**, *108*, 1163–1167.

Table VI. Bond Lengths (Å) in [Fe(OEP)(3-Cl-py)]ClO<sub>4</sub>

Fe-N(1)	1.980 (5)	C(b3)-C(b4)	1.361 (9)
Fe-N(2)	1.973 (5)	C(b5)-C(b6)	1.333 (9)
Fe-N(3)	1.976 (5)	C(b7)-C(b8)	1.356 (9)
Fe-N(4)	1.987 (5)	C(11)-C(b1)	1.682 (17)
Fe-N(5)	2.126 (5)	C(11)-C(12)	1.338 (22)
N(1)-C(a1)	1.398 (8)	C(21)-C(b2)	1.486 (9)
N(1)-C(a2)	1.370 (7)	C(21)-C(22)	1.514 (12)
N(2)-C(a3)	1.374 (7)	C(31)-C(b3)	1.488 (9)
N(2)-C(a4)	1.397 (8)	C(31)-C(32)	1.481 (11)
N(3)-C(a5)	1.394 (8)	C(41)-C(b4)	1.500 (9)
N(3)-C(a6)	1.385 (7)	C(41)-C(42)	1.531 (12)
N(4)-C(a7)	1.369 (7)	C(51)-C(b5)	1.509 (10)
N(4)-C(a8)	1.406 (8)	C(51)-C(52)	1.457 (10)
N(5)-C(1)	1.324 (9)	C(61)-c(b6)	1.491 (9)
N(5)-C(5)	1.340 (8)	C(61)-C(62)	1.495 (11)
C(a1)-c(b1)	1.453 (9)	C(71)-C(b7)	1.503 (8)
C(a1)-C(m1)	1.364 (8)	C(71)-C(72)	1.497 (10)
C(a2)-c(b2)	1.444 (9)	C(81)-C(8b)	1.498 (10)
C(a2)-C(m2)	1.368 (8)	C(81)-C(82)	1.466 (12)
C(a3)-C(b3)	1.429 (8)	C(1)-C(2)	1.391 (10)
C(a3)-C(m2)	1.377 (8)	C(2)-C(3)	1.415 (11)
C(a4)-C(b4)	1.453 (8)	C(3)-C(4)	1.372 (10)
C(a4)-C(m3)	1.372 (8)	C(4)-Cl(1)	1.724 (7)
C(a5)-C(b5)	1.460 (9)	C(4)-C(5)	1.362 (9)
C(a5)-C(m3)	1.357 (8)	Cl(2)-O(1)	1.352 (28)
C(a6)-C(b6)	1.429 (9)	Cl(2)-O(2)	1.40 (4)
C(a6)-C(m4)	1.384 (9)	Cl(2)-O(3)	1.311 (27)
C(a7)-C(b7)	1.430 (9)	Cl(2)-O(4)	1.363 (24)
C(a7)-C(m4)	1.362 (9)	Cl(2)-O(5)	1.388 (17)
C(a8)-C(b8)	1.443 (8)	Cl(2)-O(6)	1.400 (22)
C(a8)-C(m1)	1.377 (9)	Cl(2)-O(7)	1.397 (29)
C(b1)-C(b2)	1.356 (9)	Cl(2)-O(8)	1.500 (21)

<sup>a</sup>The numbers in parentheses are the estimated standard deviations.

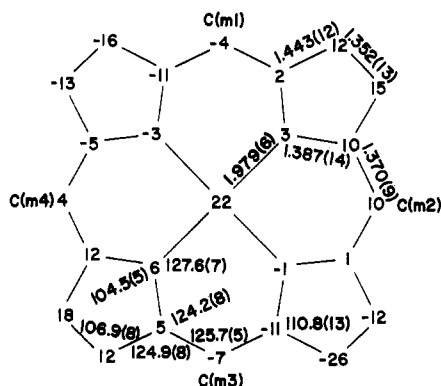


Figure 6. Formal diagram of the porphinato core in [Fe(OEP)(3-Cl-py)]ClO<sub>4</sub> displaying the deviation from the mean plane of the porphinato core (units of 0.01 Å). Values of positive displacement are toward the single axial pyridine ligand. Uncertainties in displacements are about 0.006–0.007 Å. Averaged values of bond parameters are also displayed.

are typical of ferric iron in the admixed intermediate-spin state. Finally, it should be noted that the lack of an EPR signal is consistent with the presence of  $\pi$ - $\pi$  dimers in the solid state.

Individual bond distances and angles for [Fe(OEP)(3-Cl-py)]ClO<sub>4</sub> are listed in Tables VI and VII. Averaged values for the classes in the core are displayed in Figure 6. Figure 6 also displays the conformation of the porphinato core. The core shows a modest amount of *S*<sub>4</sub> ruffling, but this is somewhat larger in magnitude than that observed in other  $\pi$ - $\pi$  dimers.<sup>28</sup> For example, the largest deviation from the mean 24-atom plane of [Fe(OEP)(2-MeHIm)<sub>2</sub>]ClO<sub>4</sub> is 0.05 Å. As is usual, individual pyrrole rings and the pyridine ligand ring are planar to within 0.01 Å.

The average Fe-N<sub>py</sub> bond distance is 1.979 (6) Å. The displacement of the iron(III) atom from the mean plane of the core is 0.22 Å. Again the structural parameters are those appropriate

Table VII. Bond Angles (deg) in [Fe(OEP)(3-Cl-py)]ClO<sub>4</sub>

N(1)FeN(2)	88.84 (20)	C(b3)C(b4)C(41)	129.0 (6)
N(1)FeN(3)	169.93 (21)	C(a5)C(b5)C(b6)	107.5 (6)
N(1)FeN(4)	90.32 (21)	C(a5)C(b5)C(51)	123.8 (6)
N(1)FeN(5)	93.29 (20)	C(b6)C(b5)C(51)	128.8 (6)
N(2)FeN(3)	89.20 (20)	C(a6)C(b6)C(b5)	106.9 (6)
N(2)FeN(4)	166.12 (21)	C(a6)C(b6)C(61)	124.5 (6)
N(2)FeN(5)	98.14 (20)	C(b5)C(b6)C(61)	128.5 (7)
N(3)FeN(4)	88.50 (21)	C(a7)C(b7)C(b8)	107.0 (6)
N(3)FeN(5)	96.78 (20)	C(a7)C(b7)C(71)	124.8 (7)
N(4)FeN(5)	95.74 (21)	C(b8)C(b7)C(71)	128.1 (7)
FeN(1)C(a1)	126.8 (4)	C(a8)C(b8)C(b7)	107.0 (6)
FeN(1)C(a2)	127.8 (4)	C(a8)C(b8)C(81)	124.0 (7)
C(a1)N(1)C(a2)	104.8 (5)	C(b7)C(b8)C(81)	129.0 (6)
FeN(2)C(a3)	127.9 (4)	C(a1)C(m1)C(a8)	125.2 (6)
FeN(2)C(a4)	127.3 (4)	C(a2)C(m2)C(a3)	125.5 (6)
C(a3)N(2)C(a4)	104.5 (4)	C(a4)C(m3)C(a5)	125.8 (6)
FeN(3)C(a5)	127.3 (4)	C(a6)C(m4)C(a7)	126.4 (6)
FeN(3)C(a6)	128.4 (4)	C(b1)C(11)C(12)	91.4 (14)
C(a5)N(3)C(a6)	103.8 (5)	C(b2)C(21)C(22)	113.0 (7)
FeN(4)C(a7)	128.6 (5)	C(b3)C(31)C(32)	112.7 (6)
FeN(4)C(a8)	126.6 (4)	C(b4)C(41)C(42)	110.7 (6)
C(a7)N(4)C(a8)	104.7 (5)	C(b5)C(51)C(52)	112.4 (7)
FeN(5)C(1)	122.2 (5)	C(b6)C(61)C(62)	113.2 (6)
FeN(5)C(5)	119.5 (4)	C(b7)C(71)C(72)	114.0 (6)
C(1)N(5)C(5)	118.0 (6)	C(b8)C(81)C(82)	114.8 (7)
N(1)C(a1)C(b1)	109.2 (5)	N(5)C(1)C(2)	124.2 (7)
N(1)C(a1)C(m1)	125.3 (6)	C(1)C(2)C(3)	116.4 (7)
C(b1)C(a1)C(m1)	125.5 (6)	C(2)C(3)C(4)	118.8 (7)
N(1)C(a2)C(b2)	112.4 (6)	C(3)C(4)C(5)	120.0 (7)
N(1)C(a2)C(m2)	124.1 (6)	C(3)C(4)Cl(1)	120.3 (7)
C(b2)C(a2)C(m2)	123.6 (6)	C(5)C(4)Cl(1)	119.7 (6)
N(2)C(a2)C(b3)	111.9 (6)	C(4)C(5)N(5)	122.6 (6)
N(2)C(a2)C(m2)	124.1 (6)	O(1)Cl(2)O(2)	96.3 (23)
C(b3)C(a3)C(m2)	124.0 (6)	O(1)Cl(2)O(3)	106.8 (20)
N(2)C(a4)C(b4)	109.5 (5)	O(1)Cl(2)O(4)	123.3 (20)
N(2)C(a4)C(m3)	124.5 (6)	O(1)Cl(2)O(5)	36.4 (19)
C(b4)C(a4)C(m3)	125.6 (6)	O(1)Cl(2)O(6)	117.0 (20)
N(3)C(a5)C(b5)	109.8 (5)	O(1)Cl(2)O(7)	74.1 (19)
N(3)C(a5)C(m3)	124.4 (6)	O(1)Cl(2)O(8)	130.6 (18)
C(b5)C(a5)C(m3)	125.8 (7)	O(2)Cl(2)O(3)	101.9 (24)
N(3)C(a6)C(b6)	112.0 (6)	O(2)Cl(2)O(4)	109.7 (17)
N(3)C(a6)C(m4)	122.7 (6)	O(2)Cl(2)O(5)	105.9 (18)
C(b6)C(a6)C(m4)	125.2 (6)	O(2)Cl(2)O(6)	24.6 (21)
N(4)C(a7)C(b7)	111.6 (6)	O(2)Cl(2)O(7)	94.0 (21)
N(4)C(a7)C(m4)	123.9 (6)	O(2)Cl(2)O(8)	132.5 (17)
C(b7)C(a7)C(m4)	124.5 (6)	O(3)Cl(2)O(4)	115.1 (20)
N(4)C(a8)C(b8)	109.7 (6)	O(3)Cl(2)O(5)	135.2 (20)
N(4)C(a8)C(m1)	124.9 (6)	O(3)Cl(2)O(6)	106.2 (22)
C(b8)C(a8)C(m1)	125.1 (7)	O(3)Cl(2)O(7)	34.9 (18)
C(a1)C(b1)C(b2)	108.2 (6)	O(3)Cl(2)O(8)	74.1 (18)
C(a1)C(b1)C(11)	124.5 (7)	O(4)Cl(2)O(5)	87.4 (15)
C(b2)C(b1)C(11)	125.6 (7)	O(4)Cl(2)O(6)	86.4 (16)
C(a2)C(b2)C(b1)	105.4 (6)	O(4)Cl(2)O(7)	147.1 (19)
C(a2)C(b2)C(21)	126.5 (6)	O(4)Cl(2)O(8)	42.8 (10)
C(b1)C(b2)C(21)	128.0 (6)	O(5)Cl(2)O(6)	113.8 (14)
C(a3)C(b3)C(b4)	106.8 (6)	O(5)Cl(2)O(7)	108.2 (16)
C(a3)C(b3)C(31)	126.0 (6)	O(5)Cl(2)O(8)	109.1 (11)
C(b4)C(b3)C(31)	126.9 (6)	O(6)Cl(2)O(7)	111.6 (19)
C(a4)C(b4)C(b3)	106.6 (6)	O(6)Cl(2)O(8)	109.4 (15)
C(a4)C(b4)C(41)	124.4 (6)	O(7)Cl(2)O(8)	104.3 (15)

<sup>a</sup>The numbers in parentheses are the estimated standard deviations.

for an admixed intermediate-spin species. Both values are in the middle of the range previously observed<sup>8,13,14,29</sup> for five-coordinate admixed intermediate-spin iron(III) porphyrinates. The ranges of values observed are 1.961–2.001 Å for Fe-N<sub>py</sub> and 0.10–0.30 Å for the displacements of the iron atom.

The dihedral angle between the pyridine plane and the coordinate plane containing N(2), N(4), and Fe is 41.1°. A most important feature of the large  $\phi$  value is the fact that there can be no significant stereochemical constraints on the axial bond distance. The axial Fe-N<sub>py</sub> bond distance of 2.126 (5) Å can be

compared with the same type of bond in six-coordinate species with all three possible spin states. The previously determined values<sup>10,11</sup> are 2.310 Å for intermediate-spin, 2.316 Å for high-spin, and 2.043 Å for low-spin bond lengths. The value in this five-coordinate complex thus maintains a trend that was first noted<sup>30</sup> in five-coordinate high-spin(III) complexes with axial anionic ligands. In these complexes, the axial bond is much shorter than expected. However, unlike the case for the high-spin species with an anionic ligand, the observed distance in [Fe(OEP)(3-Cl-py)]ClO<sub>4</sub> is not quite as short as that appropriate for a low-spin species. This has also been observed in high-spin [Fe(OEP)(2-MeHIm)]ClO<sub>4</sub>;<sup>4</sup> the axial bond distance in this complex is substantially shorter than the analogous bond distance in the high-spin six-coordinate species but is still longer than the expected low-spin distance. The axial bond length in [Fe(OEP)(3-Cl-py)]ClO<sub>4</sub> is longer than the 2.068 (4) Å value found in [Fe(OEP)(2-MeHIm)]ClO<sub>4</sub>. This parallels the usual pattern that has been observed in metalloporphyrin species; namely, axial imidazole bonds are always shorter than axial pyridine bonds. The reason for the phenomenon is not clear; we have discussed the matter briefly elsewhere.<sup>31</sup>

(30) Hoard, J. L. In *Structural Chemistry and Molecular Biology*; Rich, A., Davidson, N., Eds.; W. H. Freeman: San Francisco, CA; 1968; pp 573-594.

(31) Brennan, T. A.; Scheidt, W. R., submitted for publication.

The perchlorate ion in both complexes is located close to an axial pyridine ligand. In [Fe(OEP)(3-Cl-py)]ClO<sub>4</sub>, the interaction is reasonably tight with the closest approach of a perchlorate oxygen atom to a pyridine carbon atom of O...C = 3.2 Å. The separations in [Fe(OEP)(3-Cl-py)<sub>2</sub>]ClO<sub>4</sub> are about 0.1 Å larger.

**Summary.** Reaction of equimolar quantities of 3-chloropyridine and [Fe(OEP)(OCIO<sub>3</sub>)] has been found to lead to the simultaneous preparation of crystalline five-coordinate [Fe(OEP)(3-Cl-py)]ClO<sub>4</sub> and to a new phase of the previously characterized bis(3-chloropyridine) complex. The mono(pyridine) complex can apparently be prepared because of the formation of  $\pi$ - $\pi$  dimers. These dimers, observed in the solid state, are also thought to persist in solution. The magnetic susceptibilities and Mössbauer spectra of this admixed intermediate-spin compound are modulated by exchange interactions between magnetic centers in the dimer.

**Acknowledgment.** We are grateful for support from the National Institutes of Health (Grant HL-15627 to W.R.S. and Grant HL-16860 to G.L.) and the National Science Foundation (Grant CHE85-19913 to C.A.R.) for this research.

**Supplementary Material Available:** Tables IS and IIS, listing anisotropic temperature factors and fixed hydrogen atom positions, respectively, for [Fe(OEP)(3-Cl-py)]ClO<sub>4</sub>, and Tables IIIS and IVS, listing anisotropic temperature factors and fixed hydrogen atom positions, respectively, for [Fe(OEP)(3-Cl-py)<sub>2</sub>]ClO<sub>4</sub> (6 pages); tables of calculated and observed structure factors ( $\times 10$ ) (32 pages). Ordering information is given on any current masthead page.

Contribution from the Departamento de Química Inorgánica, Facultad de Química, Universidad de Oviedo, c/Calvo Sotelo s/n, Oviedo, Spain

## Lamellar Inorganic Ion Exchangers. H<sup>+</sup>/Ca<sup>2+</sup> Ion Exchange in $\gamma$ -Titanium Phosphate

Celia Alvarez, Ricardo Llavona, José R. Garcia, Marta Suárez, and Julio Rodriguez\*

Received August 19, 1986

The H<sup>+</sup>/Ca<sup>2+</sup> ion-exchange process was studied. Exchange isotherms and titration and hydrolysis curves were obtained at 5.0, 25.0, 40.0, and 55.0 ( $\pm 0.1$ ) °C. The TiH<sub>1.25</sub>Ca<sub>0.37</sub>(PO<sub>4</sub>)<sub>2</sub>·3.5H<sub>2</sub>O (13.1 Å) phase was formed by using CaCl<sub>2</sub> + HCl solutions. Equilibrium constants, free energy, enthalpy, and entropy of the exchange reaction were determined. The ion-exchange process and the thermal behavior of the exchanged solids were followed by X-ray diffraction. When the temperature was increased, the TiH<sub>1.25</sub>Ca<sub>0.37</sub>(PO<sub>4</sub>)<sub>2</sub>·3.5H<sub>2</sub>O (13.1 Å) phase was transformed into the TiH<sub>1.25</sub>Ca<sub>0.37</sub>(PO<sub>4</sub>)<sub>2</sub>·H<sub>2</sub>O (10.9 Å) phase and subsequently into the TiH<sub>1.25</sub>Ca<sub>0.37</sub>(PO<sub>4</sub>)<sub>2</sub> (10.2 Å) phase originating at  $T > 200$  °C mixtures of Ti(HPO<sub>4</sub>)<sub>2</sub> (9.1 Å) and TiHCa<sub>0.5</sub>(PO<sub>4</sub>)<sub>2</sub> (10.2 Å) phases. Conversions higher than 37.5% with partial decomposition of  $\gamma$ -TiP and precipitation of calcium phosphate were obtained by using CaCl<sub>2</sub> + Ca(OH)<sub>2</sub> solutions. The hydrolysis increased with temperature.

### Introduction

The phosphates of polyvalent metals are very interesting due to their ion-exchange properties. Several studies on their amorphous<sup>1</sup> and crystalline<sup>2,3</sup> forms have been performed. Among the latter, the  $\alpha$ - and  $\gamma$ -varieties of zirconium and titanium phosphates are the most widely studied.<sup>4-7</sup> The structure of  $\alpha$ -ZrP is known.<sup>8,9</sup>  $\alpha$ -ZrP and  $\alpha$ -TiP are lamellar solids with monoclinic

symmetry and a basal spacing of 7.6 Å. The structure of the  $\gamma$ -variety is not solved, but its symmetry is also monoclinic<sup>10,11</sup> and the structural arrangement is layered with basal spacings of 12.2 Å ( $\gamma$ -ZrP) and 11.6 Å ( $\gamma$ -TiP).

Lamellar phosphates have many potential applications in renal dialysis, water softening, chromatography, catalysis, membranes, and solid electrolytes fields.<sup>3</sup>

The exchange of alkaline-earth-metal cations in lamellar phosphates has received considerable attention.<sup>12-15</sup> Alberti et

(1) Amphlett, C. B. *Inorganic Ion Exchangers*; Elsevier: Amsterdam, 1964.

(2) Clearfield, A.; Nancollas, G. H.; Blessing, R. H. In *Ion Exchange and Solvent Extraction*; Marinsky, J. A., Marcus, Y., Eds.; Marcel Dekker: New York, 1983; Vol. 5.

(3) *Inorganic Ion Exchange Materials*; Clearfield, A., Ed.; CRC Press: Boca Raton, FL, 1982.

(4) Clearfield, A.; Stynes, J. A. *J. Inorg. Nucl. Chem.* **1964**, *26*, 117.

(5) Alberti, G.; Cardini-Galli, P.; Costantino, U.; Torraca, E. *J. Inorg. Nucl. Chem.* **1967**, *29*, 571.

(6) Clearfield, A.; Blessing, R. H.; Stynes, J. A. *J. Inorg. Nucl. Chem.* **1968**, *30*, 2249.

(7) Allulli, S.; Ferragina, C.; La Ginestra, A.; Massucci, M. A.; Tomassini, N. *J. Inorg. Nucl. Chem.* **1977**, *39*, 1043.

(8) Clearfield, A.; Smith, G. D. *Inorg. Chem.* **1969**, *8*, 431.

(9) Troup, J. M.; Clearfield, A. *Inorg. Chem.* **1977**, *16*, 3311.

(10) Yamanaka, S.; Tanaka, M. *J. Inorg. Nucl. Chem.* **1979**, *41*, 45.

(11) Kobayashi, E.; Yamazaki, S. *Bull. Chem. Soc. Jpn.* **1983**, *56*, 1632.

(12) Alberti, G.; Costantino, U.; Pelliccioni, M. *J. Inorg. Nucl. Chem.* **1973**, *35*, 1327.

(13) Clearfield, A.; Djuric, Z. *J. Inorg. Nucl. Chem.* **1979**, *41*, 885.

(14) Alfonso, B. F.; Suárez, M.; Garcia, J. R.; Rodriguez, J. *Mater. Chem. Phys.* **1984**, *10*, 393.

(15) Alberti, G.; Costantino, U.; Luciani, M. L. *J. Chromatogr.* **1980**, *201*, 175.